Supplementary Information (SI)

For

A highly sensitive fluorescent probe for detection of hydrazine in gas and solution phase based on the Gabriel mechanism and its bioimaging

Rajkishor Maji,[a] Ajit Kumar Mahapatra[*],[a] Kalipada Maiti,[a] Sanchita Mondal,[a] Syed Samim Ali,[a] Prithidipa Sahoo [b], Sukhendu Mandal,[c] Md Raihan Uddin [c], Shyamaprosad Goswami,[a] Ching Kheng Quah[d] and Hoong-Kun Fun[d,e]

[a]*Department of Chemistry, Indian Institute of Engineering Science and Technology, Shibpur, Howrah-711103, West Bengal, India.*

[b]*Department of Chemistry, Visva-Bharati (A Central University), Santiniketan, 731235, India.*

[c]*Department of Microbiology,University of Calcutta, Kolkata-700019, India.*

[d]*X-ray Crystallography Unit, School of Physics, Universiti Sains Malaysia, 11800 USM, Penang, Malaysia.*

[e]*Department of Pharmaceutical Chemistry College of Pharmacy, King Saud University, P.O. Box. 2457 , Riyadh 11451 Kingdom of Saudi Arabia.*

[*]Corresponding author. Fax: +91 33 26684564; Tel: +91 33 2668 4561;

E-mail: mahapatra574@gmail.com (A. K. Mahapatra)

Table of Contents:

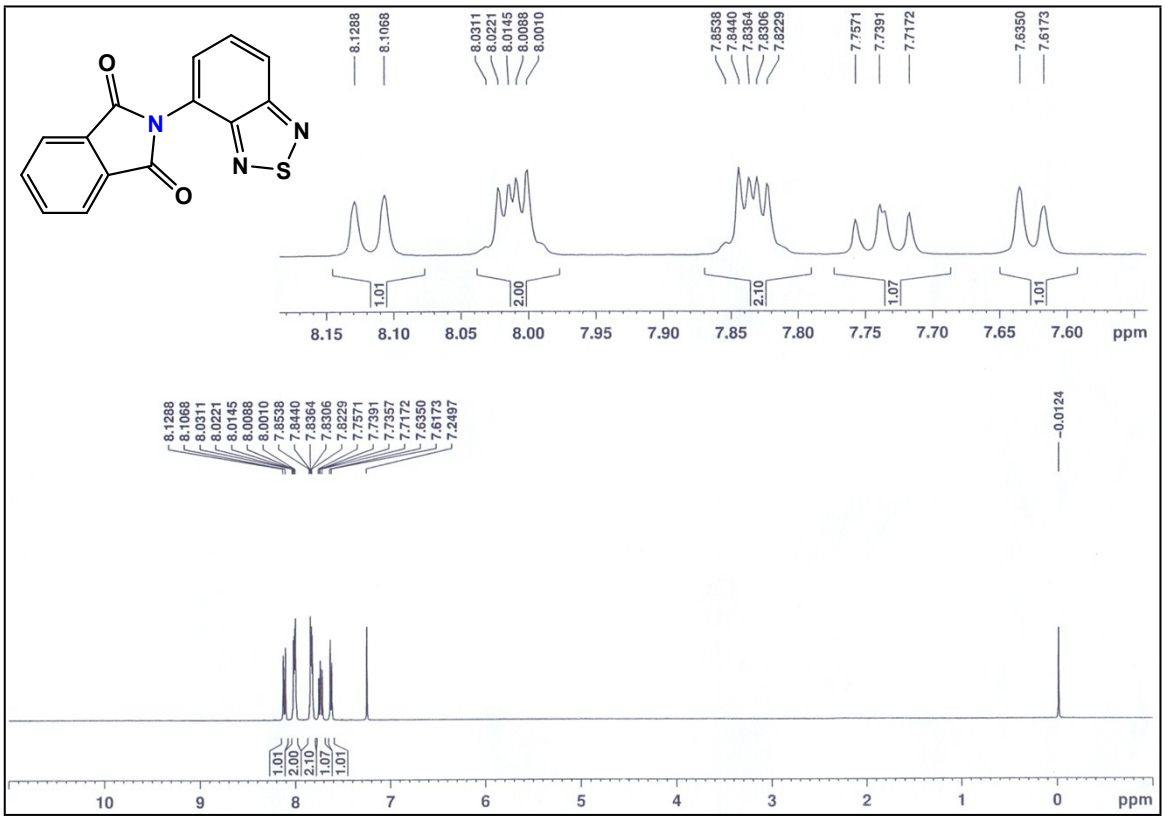

Figure S1. ^{1}H NMR of Compound **(BTI)** ($CDCl_3$, 400 MHz).

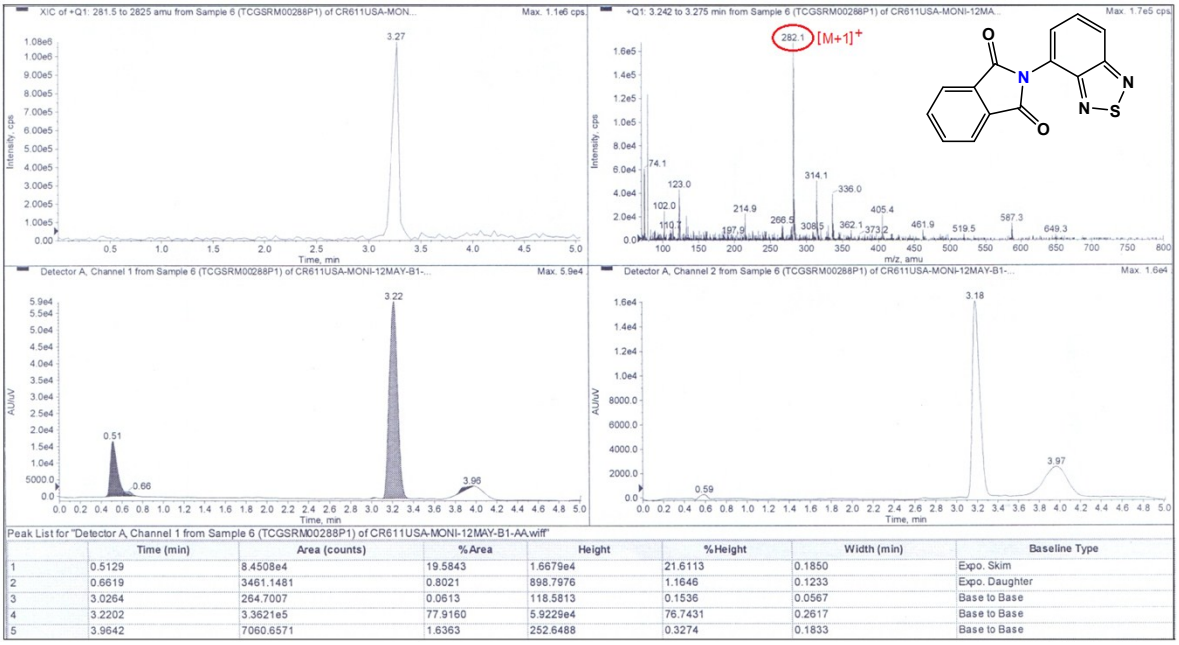

Peak List for "Detector A, Channel 1 from Sample 6 (TCGSRM00288P1) of CR611USA-MONI-12MAY-B1-AA.wiff"

	Time (min)	Area (counts)	%Area	Height	%Height	Width (min)	Baseline Type
1	0.5129	8.4508e4	19.5843	1.6679e4	21.6113	0.1850	Expo. Skim
2	0.6619	3461.1481	0.8021	898.7976	1.1646	0.1233	Expo. Daughter
3	3.0264	264.7007	0.0613	118.5813	0.1536	0.0567	Base to Base
4	3.2202	3.3621e5	77.9160	5.9229e4	76.7431	0.2617	Base to Base
5	3.9642	7060.6571	1.6363	252.6488	0.3274	0.1833	Base to Base

Figure S2. ESI LCMS spectra of Compound **(BTI)**.

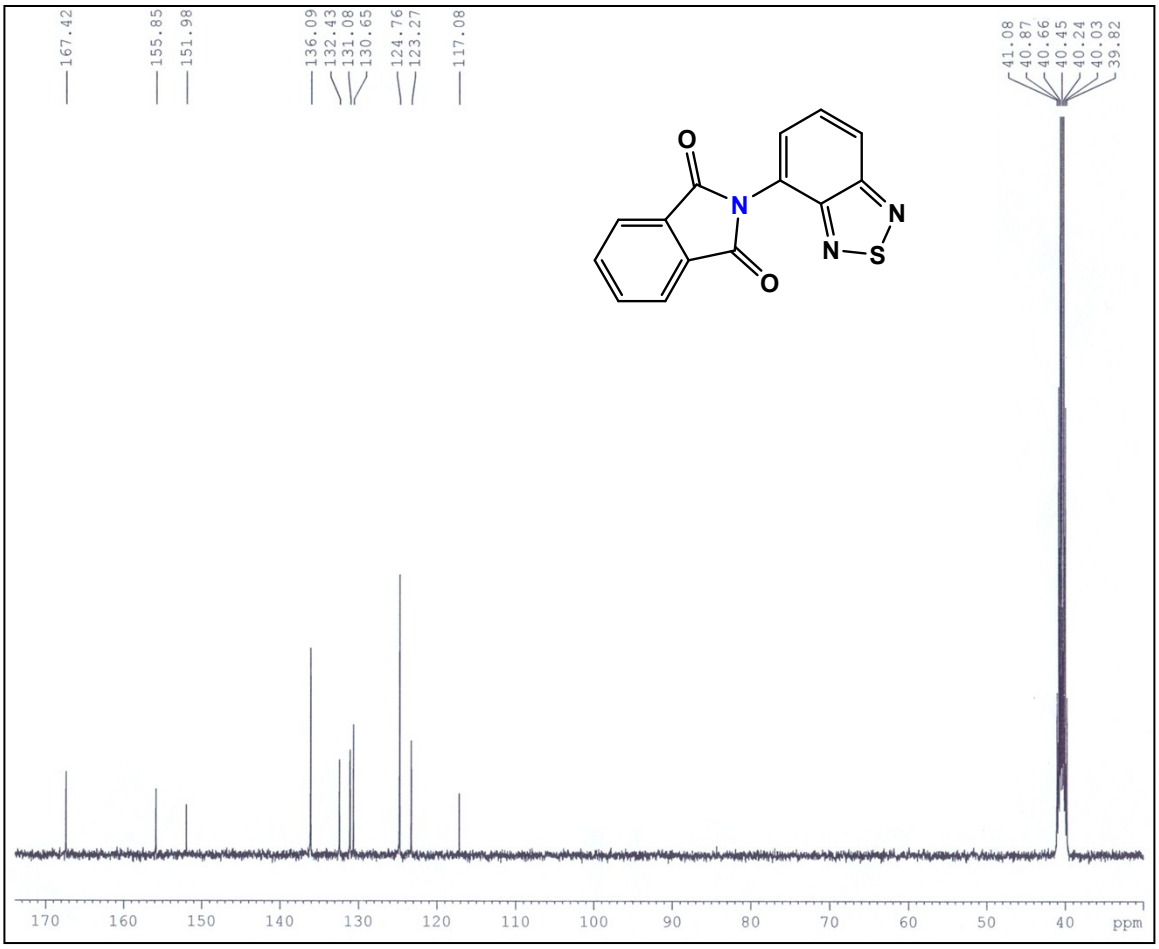

Figure S3. ^{13}C NMR spectrum of Compound **(BTI)** (DMSO-d_6, 100 MHz).

X-ray crystallography study

Crystal structure of the **BTI** was determined by single crystal X-ray diffraction from data collected at 100 K. A single crystal of 0.40 × 0.33 × 0.32 mm^3 in size was mounted on a glass fibre with epoxy cement for X-ray crystallographic study. The data were collected using a Bruker APEX2 DUO CCD diffractometer with the graphite monochromated MoKα radiation at a detector distance of 5cm and with APEX2 software. The collected data were reduced using SAINT program and the empirical absorption corrections were performed using the SADABS program. The structure were solved by direct methods and refined by least-squares using the SHELXTL software package. All non-hydrogen atoms were refined anisotropically whereas hydrogen atoms were refined isotropically. All hydrogen atoms were positioned geometrically with U_{iso} (H) = 1.2 U_{eq} (C). Crystallographic data for **BTI** are presented in Table S1 and has been deposited with the Cambridge Crystallographic Data Center No. CCDC 1479814.

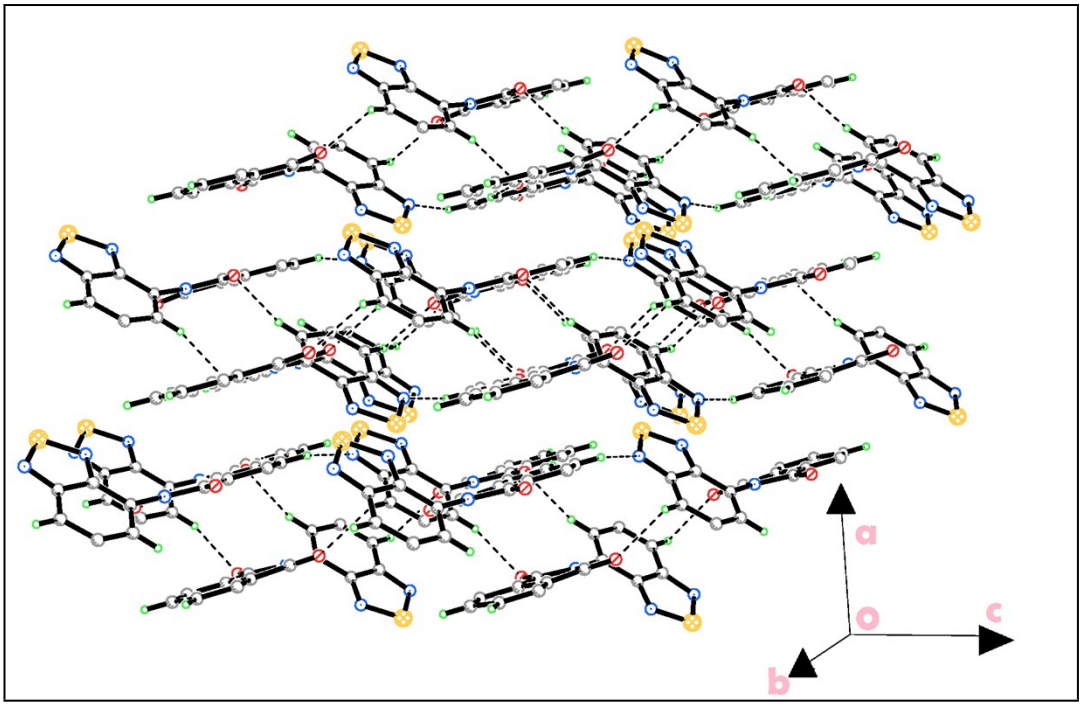

Figure S4. The crystal packing, viewed along the *b* axis, showing the molecules are linked into two-dimensional planes.

Table S1: X-ray crystallographic data

Crystal data for BTI (CCDC 1479814)	
Chemical formula	$C_{14}H_7N_3O_2S$
M_r	281.29
Crystal system, space group	Triclinic, *P*1
Temperature (K)	100
a, *b*, *c* (Å)	7.5691 (9), 8.3593 (10), 10.1479 (12)
α, β, γ (°)	83.336 (2), 88.008 (2), 67.085 (1)
V (Å^3)	587.38 (12)
Z	2
Radiation type	Mo *K*α
μ (mm^{-1})	0.28
Crystal size (mm)	0.40 × 0.33 × 0.32
Data collection	
Diffractometer	Bruker *SMART APEX* II DUO CCD area-detector diffractometer
Absorption correction	Multi-scan (*SADABS*; Bruker, 2009)
T_{min}, T_{max}	0.895, 0.916
No. of measured, independent and observed [$I > 2\sigma(I)$] reflections	8048, 2728, 2434
R_{int}	0.044
$(\sin \theta/\lambda)_{max}$ (Å^{-1})	0.655
Refinement	
$R[F^2 > 2\sigma(F^2)]$, $wR(F^2)$, S	0.037, 0.096, 1.06

No. of reflections	2728
No. of parameters	181
H-atom treatment	H-atom parameters constrained
$\Delta\rho_{max}$, $\Delta\rho_{min}$ (e Å^{-3})	0.45, −0.31

Table S2: Hydrogen-bond geometry (Å, º)

D—H···*A*	*D*—H	H···*A*	*D*···*A*	*D*—H···*A*
C4—H4*A*···N3^{i}	0.95	2.59	3.349 (2)	137
C5—H5*A*···O1^{ii}	0.95	2.56	3.357 (2)	141
C12—H12*A*···O2^{iii}	0.95	2.55	3.359 (2)	143
C14—H14*A*···O1^{iv}	0.95	2.43	3.335 (2)	159

Symmetry codes: (i) *x*, *y*−1, *z*+1; (ii) *x*, *y*−1, *z*; (iii) −*x*+1, −*y*+2, −*z*; (iv) −*x*+1, −*y*+2, −*z*+1.

Calculations for detection limit

The detection limit (DL) of **BTI** for hydrazine was determined from the following equation:

DL = K* Sb1/S

Where K = 2 or 3 (we take 2 in this case); Sb1 is the standard deviation of the blank solution; S is the slope of the calibration curve.

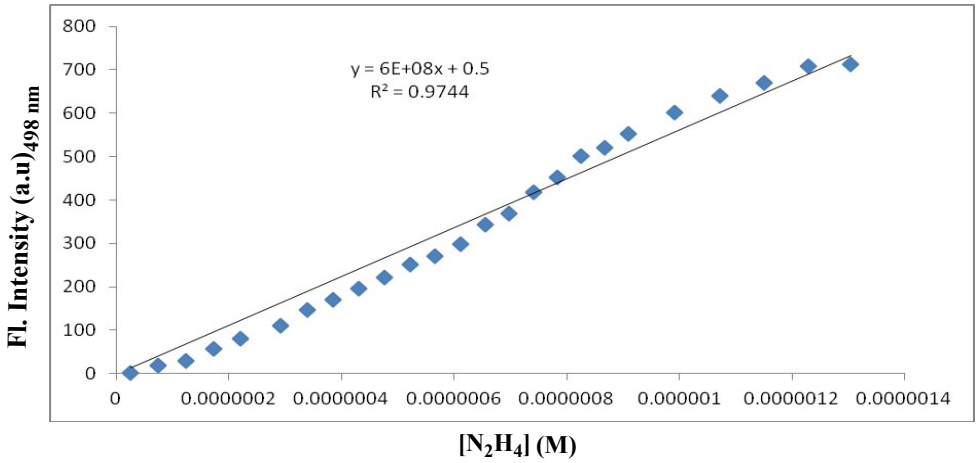

Figure S5. Calibration curve for fluorescence titration of **BTI** with hydrazine.

From the graph we get slope (S) = 6×10^{8}. Standard deviation (Sb1= 25.42144)

Thus using the formula we get the detection limit = 8.47×10^{-8} M.

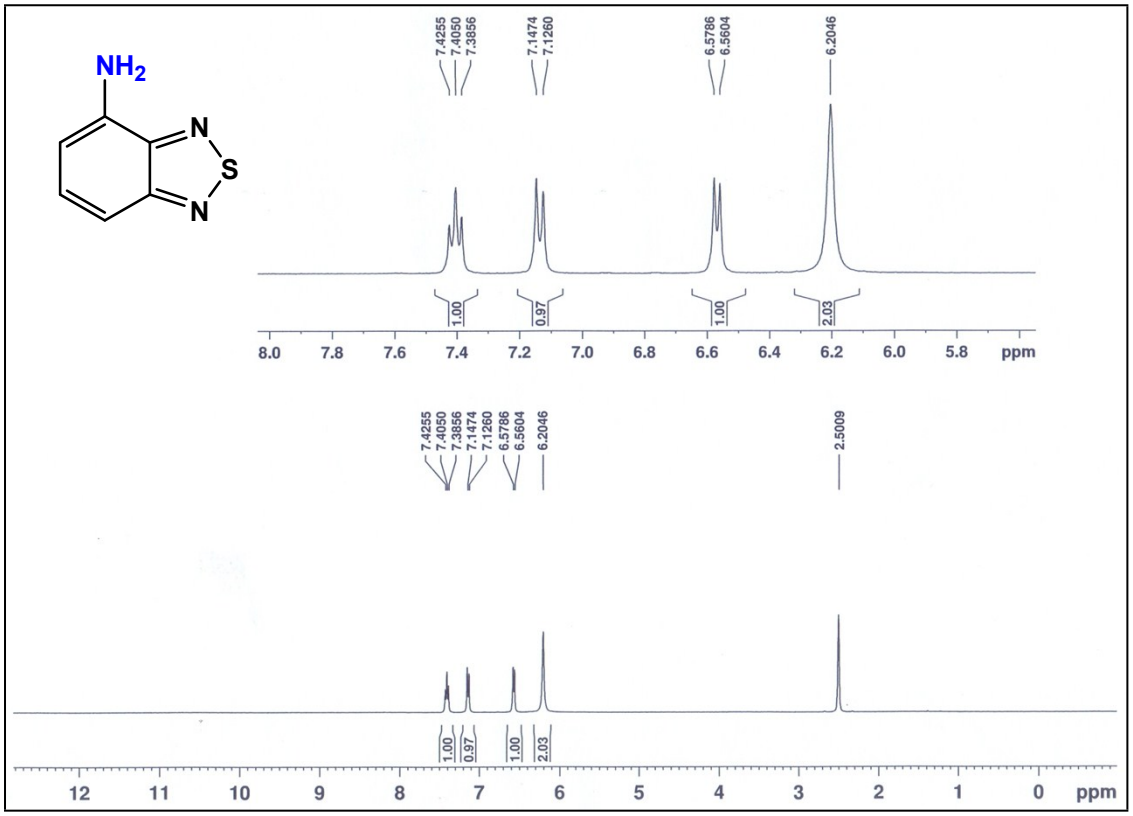

Figure S6. ^{1}H NMR of Compound **(2)** (DMSO-d_6, 400 MHz).

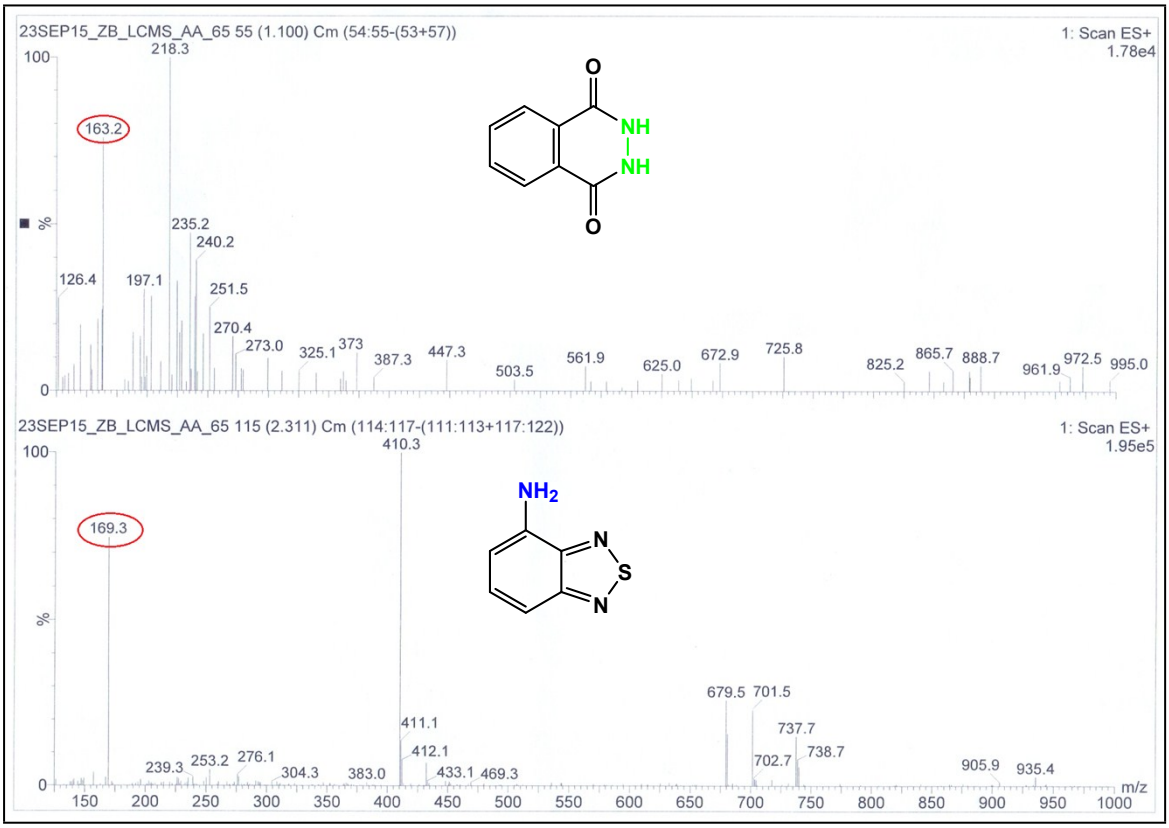

Figure S7. ESI LCMS spectra of **BTI** + N_2H_4.

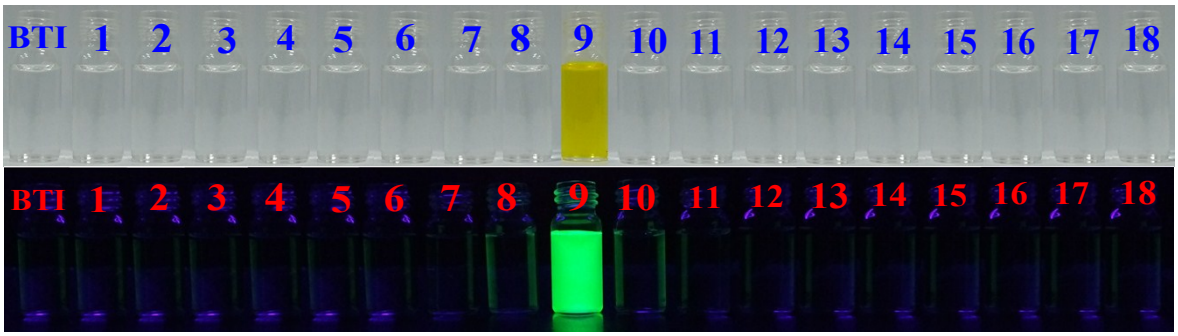

Figure S8. The photograph of visible color (top) under ambient light and visual fluorescence color (bottom) changes of sensor **BTI** (c = 1 x 10^{-6} ML^{-1}) with various relevant analytes in H_2O–DMSO (4:6, v/v) solution (10 mM HEPES buffer, pH 7.4) under a hand–held UV lamp (366 nm): **BTI** only; (1) F^-; (2) Cl^-; (3) Br^-; (4) I^-; (5) CN^-; (6) PO_4^{3-}; (7)

NO_3^- ; (8) S^{2-}; (9) hydrazine; (10) SO_4^{2-}; (11) Cu^{2+}; (12) Hg^{2+}; (13) Zn^{2+}; (14) Cd^{2+}; (15) Mg^{2+}; (16) Fe^{3+}; (17) Al^{3+}; (18) Ag^+.

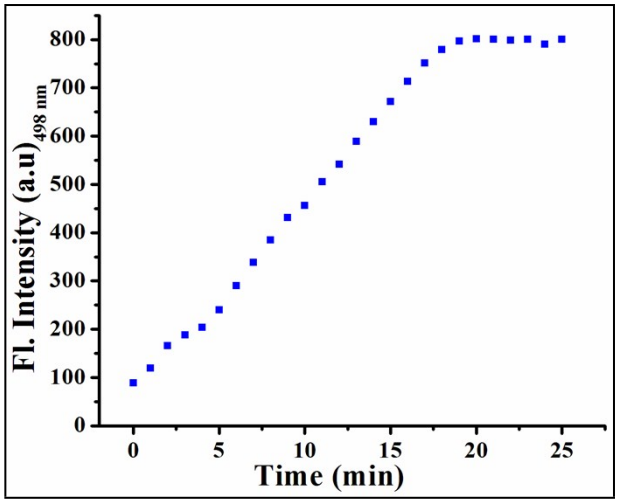

Figure S9. Time-dependent fluorescence intensity changes of probe **BTI** (c = 1 x 10^{-6} ML^{-1}) with hydrazine (1.5 equivalents) at 498 nm in H_2O–DMSO (4:6, v/v) solution (10 mM HEPES buffer, pH 7.4) at room temperature. The excitation wavelength is 313 nm.

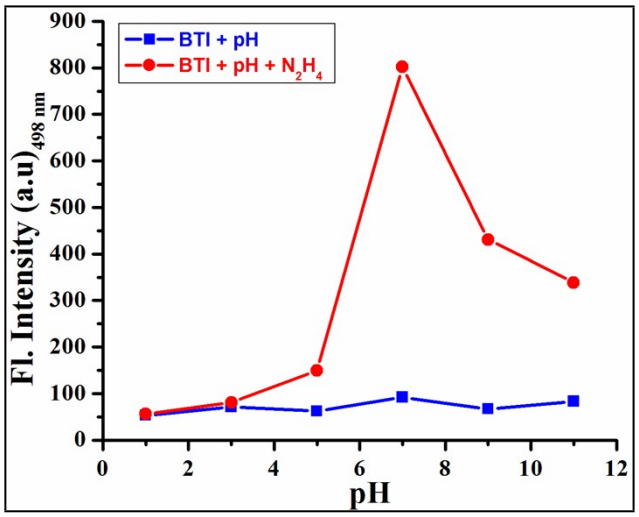

Figure S10. Fluorescence pH titration of **BTI** (c = 1 x 10^{-6} ML^{-1}) in presence (red) and absence (blue) of 1.5 equiv. of hydrazine at 498 nm in H_2O–DMSO (4:6, v/v) solution (excitation at 313 nm).

Computational details

Geometries have been optimized using the B3LYP/6-31+G(d,p) level of theory in presence of solvent water. Solvent effects were incorporated using SMD solvent model[1] implemented in Gaussian 09. The geometries are verified as proper minima by frequency calculations. Time-dependent density functional theory calculation has also been performed at the same level of theory.

Table S3. Selected electronic excitation energies (eV), oscillator strengths (f), main configurations, and CI Coefficients of the low-lying excited states of **BTI**, **2** and **3**. The data were calculated by TDDFT//B3LYP/6-31+G(*d,p*) + solv(SMD) based on the optimized ground state geometries.

Molecules	Electronic Transition	Excitation Energy[a]	f[b]	Composition[c]	(composition) %
BTI	$S_0 \rightarrow S_2$	3.6804 eV 336.87 nm	0.3052	H → L	94.4
	$S_0 \rightarrow S_6$	4.2538 eV 291.47 nm	0.1108	H-2 → L H-3 → L	86.9
	$S_0 \rightarrow S_9$	4.3875 eV 282.58 nm	0.2698	H-2 → L	66.4
	$S_0 \rightarrow S_{16}$	5.3310 eV 232.57 nm	0.2065	H-5 → L	87.6
	$S_0 \rightarrow S_{19}$	5.6643 eV 218.89 nm	0.9165	H-1 → L+1	74.6
2	$S_0 \rightarrow S_1$	2.6585 eV 466.37 nm	0.0571	H → L	98.8
	$S_0 \rightarrow S_2$	4.3857 eV 282.70 nm	0.1646	H-1 → L	82.5
	$S_0 \rightarrow S_6$	5.1995 eV 238.45 nm	0.1153	H-2 → L	80.9
	$S_0 \rightarrow S_7$	5.2435 eV 236.45 nm	0.3783	H → L+2	69.2
	$S_0 \rightarrow S_9$	5.5144 eV 224.84 nm	0.2564	H → L+4	87.6
3	$S_0 \rightarrow S_1$	4.2610 eV 290.97 nm	0.0647	H → L	97.8
	$S_0 \rightarrow S_6$	5.1963 eV 238.60 nm	0.1168	H-2 → L H-1 → L+1	93.9
	$S_0 \rightarrow S_9$	5.7301 eV 216.37 nm	0.2453	H-1 → L+1	66.8
	$S_0 \rightarrow S_{12}$	5.7734 eV 214.75 nm	0.7762	H-2 → L+1 H-1 → L	95.1

[a] Only selected excited states were considered. The numbers in parentheses are the excitation energy in wavelength. [b] Oscillator strength. [c] H stands for HOMO and L stands for LUMO.

Table S4. Energies of the highest occupied molecular orbital (HOMO) and lowest unoccupied molecular orbital (LUMO)

Species	E_{HOMO} (a.u)	E_{LUMO}(a.u)	ΔE(a.u)	ΔE(eV)	ΔE(kcal/mol)
BTI	-0.25809	-0.10478	0.15331	4.171672	96.20348
2	-0.21025	-0.09129	0.11896	3.236985	74.64853
3	-0.24453	-0.06966	0.17487	4.758335	109.7326

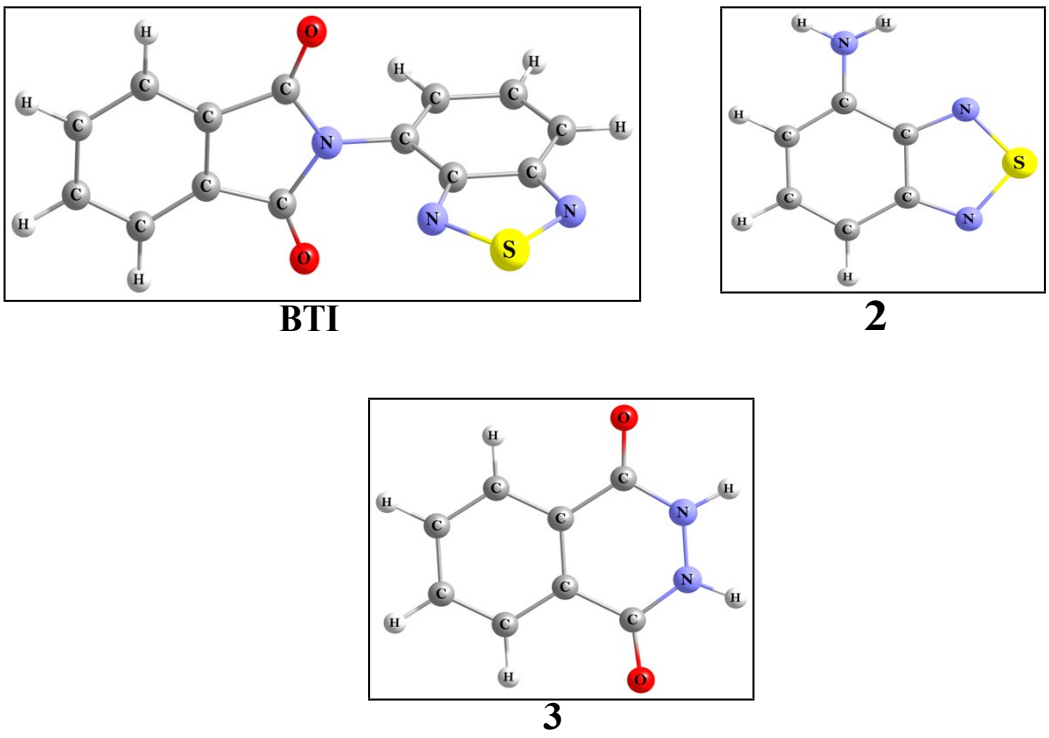

Figure S11. Optimized ground-state geometries of Compound **(BTI), 2** and **3**.

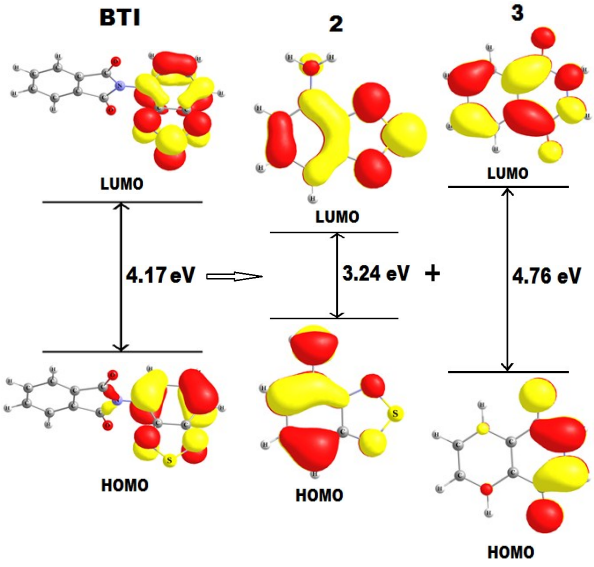

Figure S12. Calculated (TDDFT//B3LYP/6-31+G(*d,p*) + solv(SMD) level) geometry and HOMO−LUMO energy levels and the interfacial plots of the orbitals for sensor **BTI**, **2** and **3** in solvent phase.

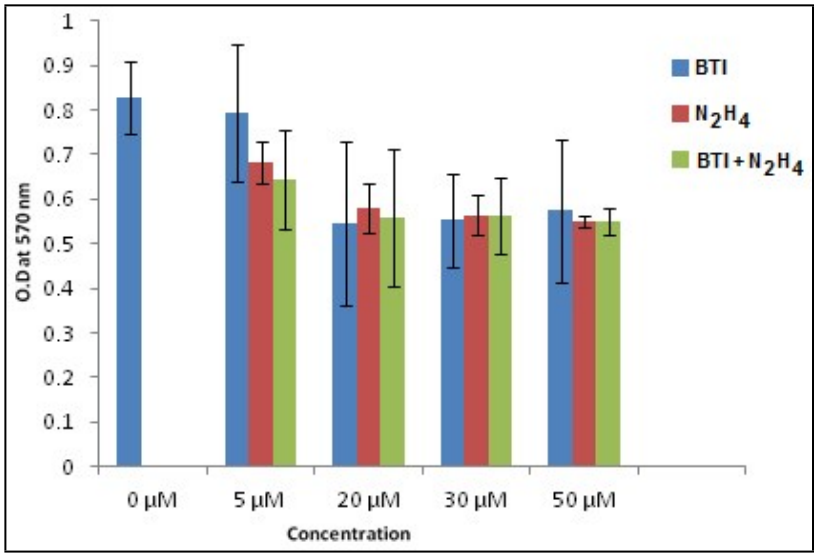

Figure S13. MTT assay to determine the cytotoxic effect of Probe **BTI** and **BTI** -N_2H_4 on Vero 76 cells (Vero 76, ATCC No CRL-1587).

Determination of quantum yield:

For measurement of the quantum yields of **BTI** and **BTI**-N_2H_4, we recorded the absorbance of the compounds in DMSO solution. The emission spectra were recorded using the maximal excitation wavelengths, and the integrated areas of the fluorescence-corrected spectra were measured. The quantum yield of **BTI** and **BTI**-N_2H_4 were then calculated by comparison with anthracene (Φs = 0.28 in EtOH) as reference using the following equation.

$\phi_x = \phi_s (F_x / F_s)(A_s / A_x)(n_x^2/ n_s^2)$

Where,

X & S indicate the unknown and standard solution respectively, ϕ = quantum yield,

F = area under the emission curve, A = absorbance at the excitation wave length,

n = index of refraction of the solvent. Here ϕ measurements were performed using anthracene in ethanol as standard [ϕ = 0.28]. Uv-vis and fluorescence titration of **BTI** in presence of hydrazine were carried out in dimethyl sulfoxide solution.

For standard (s) anthracene in ethanol the following values were determined:

n_s = 1.3614 (for ethanol); ϕ_s = 0.28.

Here for **BTI**, n_x=1.4793 (for Dimethyl Sulfoxide), (range: from 400 nm to 600 nm), we calculate the quantum yield ϕ_x (**BTI**) = 0.067.

For, **BTI**-N_2H_4, n_x=1.4793 (for Dimethyl Sulfoxide), (range: from 400 nm to 600 nm), we calculate the quantum yield ϕ_x (**BTI**-N_2H_4)= 0.704.

References:

(1) A. V. Marenich, C. J. Cramer and D. G. Truhlar, *J. Phys. Chem. B*, 2009, **113**, 6378-6396.